УДК 621.7

Yan Beygelzimer[1], Roman Kulagin[2] , Yajun J. Zhao[3,4], Laszlo S. Toth[3,4], Michail Shtern[5]
[1]Donetsk Institute for Physics and Engineering named after O.O. Galkin, National Academy of Sciences of Ukraine
[2]Institute of Nanotechnology (INT), Karlsruhe Institute of Technology (KIT), Germany
[3]Laboratory of Excellence on Design of Alloy Metals for low-mAss Structures (DAMAS), Université de Lorraine, France
[4]Laboratoire d'Etude des Microstructures et de Mécanique des Matériaux (LEM3), France
[5]Frantsevich Institute of Materials Science, National Academy of Sciences of Ukraine

MODELING OF STRAIN AND DENSITY DISTRIBUTION DURING HIGH PRESSURE TORSION OF PRE-COMPACTED POWDER MATERIALS

It is shown by finite element modeling that under high pressure torsion of water-atomized pure iron powder a zone with high shear strain and high density develops first in a layer adjacent to the moving anvil. The finite element simulation results and an analytical calculation using the minimum plastic energy extremum principle both show that with further deformation the compacted zone extends progressively in the radial and axial directions throughout the specimen.

Keywords*: high pressure torsion, powder, porosity, mathematical simulation*

Бейгельзимер Я.Е., Кулагин Р.Ю., Yajun J. Zhao, Laszlo S. Toth, М.Б. Штерн

МОДЕЛИРОВАНИЕ ДЕФОРМАЦИИ И РАСПРЕДЕЛЕНИЯ ПЛОТНОСТИ ПРИ КРУЧЕНИИ ПОД ДАВЛЕНИЕМ ПРЕДВАРИТЕЛЬНО СКОМПАКТИРОВАННЫХ ПОРОШКОВЫХ МАТЕРИАЛОВ

С помощью моделирования методом конечных элементов показано, что при кручении под давлением образца из предварительно скомпактированного порошкового железа, зона с высокой деформацией сдвига и высокой плотностью в начале процесса локализуется в слое, примыкающем к подвижной наковальне. При дальнейшей деформации уплотненная зона постепенно распространяется в радиальных и осевых направлениях по всему образцу.

Ключевые слова: *кручение под высоким давлением, порошок, пористость, математическое моделирование*

Бейгельзімер Я.Ю., Кулагін Р.Ю., Yajun J. Zhao, Laszlo S. Toth, М.Б. Штерн

МОДЕЛЮВАННЯ ДЕФОРМАЦІЇ І РОЗПОДІЛУ ГУСТИНИ ПРИ КРУЧЕННІ ПІД ТИСКОМ ПОПЕРЕДНЬО СКОМПАКТІРОВАННИХ ПОРОШКОВИХ МАТЕРІАЛІВ

За допомогою моделювання методом кінцевих елементів показано, що при крученні під тиском зразка з попередньо скомпактірованного порошкового заліза, зона з високою деформацією зсуву і високою щільністю на початку процесу локалізується в шарі, що примикає до рухомий ковадлі. При подальшій деформації ущільнена зона поступово поширюється в радіальних і осьових напрямах по всьому зразку.

Ключові слова: *кручення під високим тиском, порошок, пористість, математичне моделювання*

We dedicate this paper to 70th anniversary of Victor Rud', the wonderful person, who has opened the door to the experimental mechanics of porous and powder materials

Introduction

High pressure torsion (HPT) is the effective severe plastic deformation processes [1]. It is used for making materials with exceptionally small grain size (about 100 nm), as well as for consolidating of powder materials. In the latter case also occurs grain refinement.

Strain distribution by volume of the sample is the most important characteristic of the HPT. Recently, it was found that the strain distribution at the HPT is non-uniform not only in radial direction (it has been known from the early work on HPT), but also in axial direction of the sample [2]. Extreme heterogeneity of the strain was founded in article [3], where dead zone is shown.

The articles [4,5] present the results of experiments on the consolidation of water atomized commercially pure iron powder by true constrained high pressure torsion (by the classification of the paper [1]) (Fig.1). Because of the high hydrostatic pressure, this scheme is the best for the HPT of powder materials.

In the article [4] is shown that porosity of powder specimens decreases with saturation to about 3% under uniaxial compression. Torsion under pressure leads to a further porosity reduction up to tenths of a percent. In the paper [5] is shown that there is a considerable heterogeneity of the strain in axial direction under HPT of powders.

In this paper, we investigate theoretically HPT of powder sample under the same conditions as in the articles [4,5]. The study showed that with increasing of a rotation angle of the anvil the border of an area with a high density is spreading through the specimen. It starts from the edge of rotating piston and moves in both radial and axial directions in the sample volume. The porosity in the volume of the sample tends to a steady-state value, which is determined by the axial pressure. Comparison of the strain distribution and porosity in the sample volume for the experimental conditions [4,5] show good correspondence between theory and experiment.

Mathematical simulation

The purpose of the mathematical simulation was to study the evolution of the strain and the density distribution in the bulk of precompacted pure iron powder during it torsion under pressure.

Different rheological models is used for the simulation of plastic deformation of powder materials by finite element method [6].The most commonly used modified Drucker–Prager cap model [7] and Shima-Oyane model [8], which are offered in ABAQUS and DEFORM software . To analyze the process, we apply the model [9-11], which combines the features of the models [7] and [8], and allows one to make some conclusions about the physical mechanisms of deformation. This model takes into account both processes accompanying the plastic deformation of materials with low porosity: reduction of voids as well as the formation of new ones. The reason of the second processes is the structural heterogeneity of the material.

The model [9-11] is represented by the following equations:

$$\frac{\sigma^2}{\psi(\theta)}+\frac{\tau^2}{\varphi(\theta)}=(1-\theta)\left(k_0-\alpha\sigma\right)^2, \quad (1)$$

$$\frac{\dot{e}\tau}{\varphi(\theta)}=\dot{g}\left(\frac{\sigma}{\psi(\theta)}+\alpha(1-\theta)(k_0-\alpha\sigma)\right), \quad (2)$$

$$\dot{e}_{ij}-\frac{1}{3}\dot{e}\delta_{ij}=\frac{\dot{g}}{\tau}\left(\sigma_{ij}-\sigma\delta_{ij}\right), \quad (3)$$

where σ_{ik} and $\dot{e}_{ik}$ are the components of stress and strain rate tensors; $\sigma=\frac{1}{3}\sigma_{ik}\delta_{ik}$ and $\dot{e}=\dot{e}_{ik}\delta_{ik}$ respectively denote the hydrostatic stress and the volume strain rate; $\tau=\sqrt{\left(\left(\sigma_{ik}-\frac{1}{3}\sigma\delta_{ik}\right)\left(\sigma_{ik}-\frac{1}{3}\sigma\delta_{ik}\right)\right)}$ and $\dot{g}=\sqrt{\left(\left(\dot{e}_{ik}-\frac{1}{3}\dot{e}\,\delta_{ik}\right)\left(\dot{e}_{ik}-\frac{1}{3}\dot{e}\delta_{ik}\right)\right)}$ respectively denote stress and strain rate deviator intensity; θ-porosity, k_0, α, a, m, n - material parameters (the technique for determining the value of them and its specific values for different materials and conditions are presented in [9,11]);

$$\psi(\theta)=\frac{(1-\theta)^{2n-1}}{6a\theta^m}, \ \varphi(\theta)=(1-\theta)^{2n-1} \quad (4)$$

The parameter α is a coefficient of inner friction. According to [9, 11], it is a quantitative measure of separate structural elements' ability to accommodate each other. In the case, when complete adaptation of the elements to each other is possible, α =0. The value of α grows with the increase in the number of restrictions to the joint plastic deformation. That is, the less efficient the mechanisms of plastic deformation of the structural elements are, the higher is α.

According to the paper [4] the porosity precompacted pure iron powder close to 3% before starting of rotation of the anvil. For materials with a low porosity and compact materials the value of the α is of the order 0.01-0.001, a is of the order 0.1-0.01, and $k_0 = \sqrt{\frac{2}{3}}\sigma_s$, where σ_s is the flow stress of the basic material [9, 11]. Considering this, when $\theta << 1$, one can obtained from (1)-(4), in the first approximation, the next system of the equations:

$$\tau = k_0, \tag{5}$$

$$\frac{d\theta}{de_M} = \alpha\sqrt{\frac{3}{2}} + 9a\theta\frac{\sigma}{\sigma_s}, \tag{6}$$

$$\dot{e}_{ij} - \frac{1}{3}\dot{e}\delta_{ij} = \frac{3}{2}\frac{\dot{e}_M}{\sigma_s}\left(\sigma_{ij} - \sigma\delta_{ij}\right), \tag{7}$$

where $\dot{e}_M = \sqrt{\frac{2}{3}}\dot{g}$ - Von Mises strain rate; $e_M = \int_0^t \dot{e}_M dt$ - Von Mises strain.

According to Eqs. (5) and (7), when $\theta << 1$, in the first approximation, one can find the stress-strain state of the specimen on the base of Von Mises model for rigid-plastic incompressible materials (see, e.g. [12]) and after that the porosity of the materials can be find by solving the kinetic equation (6). The exception is when there is a loss of stability of the material with the formation of shear bands [9]. We will not consider these regimes in this article.

The problem is solved by the finite element methods using the commercial package DEFORM-2D/3D V11.0 [13]. Figure 1 shows the schematic geometry of the HPT system we used.

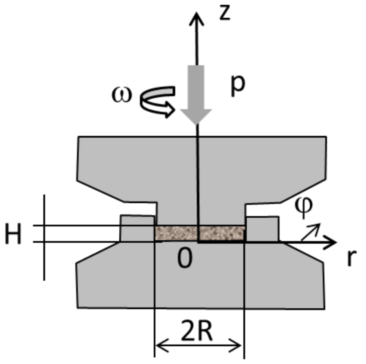

Fig.1 **The schematic geometry of the HPT system for powder consolidation**

We have took, according the paper [5]: $R = 10mm$, $H = 3mm$. According to the paper [9] we have for pure iron: $\alpha = 2.7 \cdot 10^{-3}$, $a = 2.7 \cdot 10^{-2}$. The stress–strain curve for precompacted pure iron powder we get from the paper [5].

We accept sticking on the flat surfaces of the anvils and the friction condition $\tau_f = m\sigma_s$ on the cylindrical surface, where m is the parameter of friction. We taken $m = 0.25$.

The initial number of elements of 150,000 was introduced. The upper anvil rotated at 0.1 rad s^{-1} up to a 2 full turn under a constant pressure $p = 1.1GPa$. The initial condition, according [5]: $\theta = 3.02 \cdot 10^{-2}$, when the $t = 0$.

By the calculation, we determined the strain and the porosity distributions in an axial cross-section of the specimen at different angles of rotation of the anvil. For comparison with experiment [4], we determined the average porosity of the sample calculated by the formula

$$\bar{\theta} = \frac{2\pi}{V}\int_0^H\int_0^R \theta(r,z)rdrdz \tag{8}$$

Results and Discussion

The Von Mizes strain distribution in the axial cross-section of the sample is shown on the Fig.2.

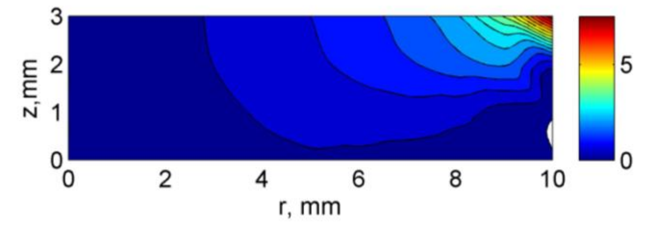

a

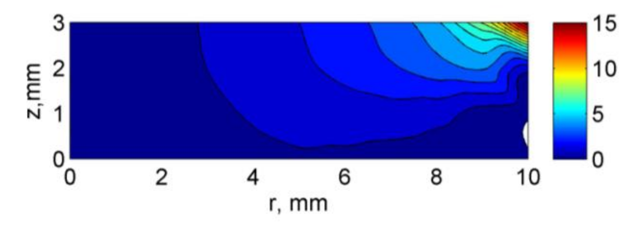

b

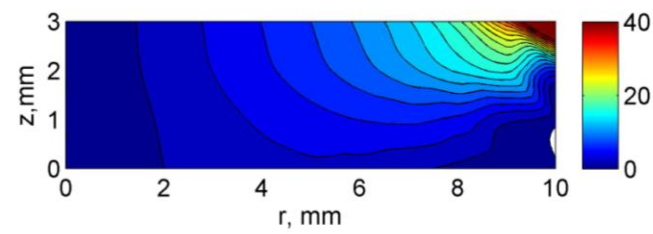

c

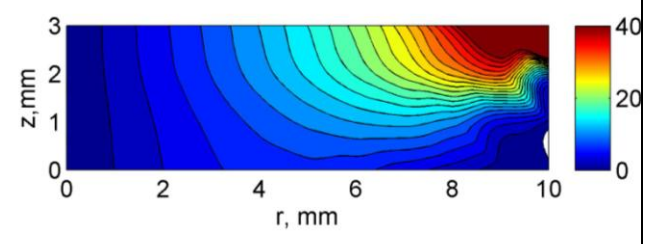

d

Fig.2 **The von Mizes strain distribution in the axial cross-section of the sample for the compression pressure** $p = 1.1GPa$ **and for the rotation angle equals to: a-** $\frac{\pi}{4}$**, b-** $\frac{\pi}{2}$**, c-** 2π **, and d-** 4π **.**

The Fig.2 shows that the HPT has a strong strain heterogeneity, not only in the radial direction, but in the axial one. This result good agrees with experiment. The calculated shear strain distribution at a distance of 9.61 mm from the axis after rotation by the angle of π/2 in comparison with the experimental one [5] are shown in Fig.3.

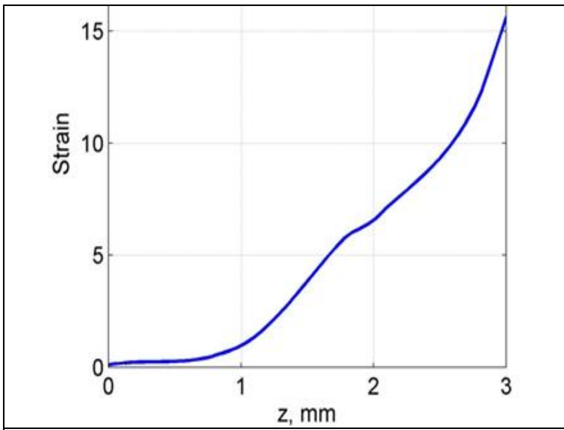

a

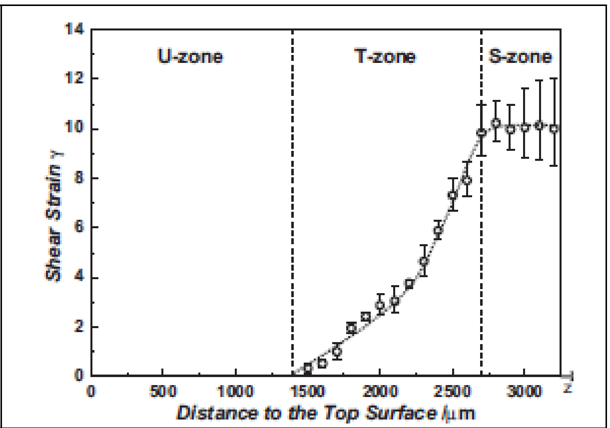

b

Fig 3. **The calculated shear strain distribution (*a*) at the distance of 9.61 mm from the axis after rotation by the angle of π/2 in comparison with the experimental one [5] (*b*).**

Let's assume the isoline with Von Mises strain equal 1 as a nominal border of a zone of large plastic deformations. The Figure 4 shows that this border moves both in the radial and axial directions with increasing rotation angle.

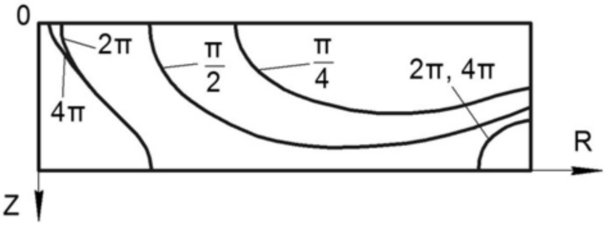

Figure 4. **The moving of the border of the zone of large plastic deformation (the isoline with Von Mises strain equal 1).**

Moving of this border in the radial direction follows from the well-known equation for Von Mises strain for HPT:

$$e_M = \frac{r\beta}{\sqrt{3}H}\ , \tag{9}$$

where β is the rotation angle of the anvil, r - is the distance from the axis z (see Fig.1).

Indeed, one can get from the Eq. (9) the radius r_1 of the isoline with Von Mises strain equal 1:

$$r_1 = \frac{\sqrt{3}H}{\beta} \tag{10}$$

One can see that r_1 really decrease when β increase.

Let's show that moving of the border in the axial direction follows from the extremum principles of the theory of plasticity in particularly from the minimum properties of an actual velocity field (see, e.g., [12]).

According to this principle, the actual velocity field minimizes the functional of power dissipation

$$W\left(\vec{V}^*\right) = \int_{\Omega} \sigma_s \dot{e}_M^* dV + \int_{S_f} \tau_f V_\tau^* dS\ , \tag{11}$$

where the first integral is taken over the volume of a deformable body, and the second - on the surface S_f of its contact with the tool where there is friction between the deformable material and tool; $\vec{V}^*$ is so-called kinematically admissible velocity field, V_τ^* is its projection to the surface S_f; τ_f - friction stress; e_M^* is Von Mises strain rate for the kinematically admissible velocity field.

Kinematically admissible velocity field must satisfy the boundary conditions for the velocity and the incompressibility condition $div\vec{V}^* = 0$ [12]. Let's take the kinematically admissible velocity field in the form

$$\vec{V}^* = \omega r \Phi(z) \vec{n}_\varphi\ , \tag{12}$$

where $\vec{n}_\varphi$ is the unit vector in the direction of the φ axis of the cylindrical coordinate system (r, φ, z) (see Fig.1); ω is the rotating rate of the upper anvil; $\Phi(z)$ -arbitrary smooth function of z, satisfies the boundary conditions:

$$\Phi(0) = 0 \text{ and } \Phi(H) = 1 \tag{13}$$

It is easy to verify by direct calculation that the field (12) satisfies the condition of incompressibility $div\vec{V}^* = 0$, and the boundary conditions for the velocity. The latter are the conditions of material sticking to the flat surfaces of the anvil and the presence of only a tangential velocity component on a cylindrical surface $r = R$.

When $\Phi(z) = \frac{z}{H}$, the Eq. (12) coincide with the velocity field usually used for HPT. We generalize this expression and take

$$\Phi(z)=\left(\frac{z}{H}\right)^k, \tag{14}$$

where k is parameter.

Let's find the k using the principle of minimum properties of an actual velocity field.

Let's introduce dimensionless variables:

$$\bar{z}=\frac{z}{H},\quad \bar{r}=\frac{r}{R},\quad \bar{\sigma}_s=\frac{\sigma_s}{\sigma_{s0}} \tag{15}$$

It is easy to prove that the Von Mises strain rate for the kinematically admissible velocity field has the form:

$$\dot{e}_M^*=\frac{\omega R\bar{r}}{\sqrt{3}H}\frac{d\Phi}{d\bar{z}}\quad , \tag{14}$$

The projection of the field (12) to the surface S_f is

$$V_\tau^*=\omega R\Phi(\bar{z})\quad , \tag{15}$$

One can obtain using Eqs.(11), (14), (15) and the friction condition $\tau_f=m\sigma_s$:

$$\frac{W}{2\pi\omega R^2 H\sigma_{s0}}=\frac{R}{\sqrt{3}H}\int_0^1 k\bar{z}^{k-1}\left[\int_0^1\bar{\sigma}_s\bar{r}^2 d\bar{r}\right]d\bar{z}+m\int_0^1\bar{\sigma}_s\bar{z}^k d\bar{z}\ , \tag{16}$$

At the start of the rotation of the anvil the flow stress of the materials is equals σ_{s0} therefore $\bar{\sigma}_s=1$ throughout the volume of the sample. One can get from the Eq. (16) for the start of the rotation of the anvil:

$$\frac{W(0,k)}{2\pi\omega R^2 H\sigma_{s0}}=\frac{R}{3\sqrt{3}H}+\frac{m\bar{z}^{k+1}}{k+1}\ , \tag{17}$$

By increasing k the right-hand side of this ratio decreases monotonically, approaching to $\dfrac{R}{3\sqrt{3}H}$ while $k\to\infty$.

The dependence $\Phi(\bar{z})=\bar{z}^k$ for $k>>1$ ($k=100$) is shown in Figure 5. It means that only thin layer of material with thickness a $\Delta\bar{z}<<1$ adjacent to the upper anvil is mainly deformed at the start of the its rotation.

The plastic deformation leads to a hardening of the materials in this layer. Because of this the specimen becomes ununiformed. Let's $\bar{\sigma}_{s1}$ is average flow stress of the hardened materials. In this case one can obtain from the Eq. (16):

$$\frac{W(\Delta\bar{z},k)}{2\pi\omega R^2 H\sigma_{s0}}=\frac{R}{3\sqrt{3}H}\left[\bar{\sigma}_{s1}k\Delta\bar{z}+(1-\Delta\bar{z})^k\right]+m\left[\bar{\sigma}_{s1}\Delta\bar{z}+\frac{(1-\Delta\bar{z})^{k+1}}{k+1}\right] \tag{18}$$

If $\Delta\bar{z}<<1$, then

$$\frac{W(\Delta\bar{z},k)}{2\pi\omega R^2 H\sigma_{s0}}=\frac{R}{3\sqrt{3}H}\left[1+k\Delta\bar{z}(\bar{\sigma}_{s1}-1)\right]+m\left[\Delta\bar{z}(\bar{\sigma}_{s1}-1)+\frac{1}{k+1}\right], \tag{19}$$

Minimum of the W is determined by the condition

$$\frac{dW(\Delta\bar{z},k)}{dk}=\frac{R}{3\sqrt{3}H}\Delta\bar{z}(\bar{\sigma}_{s1}-1)-\frac{m}{(k+1)^2}=0\ , \tag{20}$$

One can get from the Eq. (20)

$$k=\sqrt{\frac{3\sqrt{3}Hm}{R\Delta\bar{z}(\bar{\sigma}_{s1}-1)}}-1 \tag{21}$$

When hardening is weak, then $\bar{\sigma}_{s1}\to 1$ and $k\to\infty$. In this case the velocity field (12) is very heterogeneous and deformation remains localized in the top thin layer. If the material hardens rapidly, it is reduces the value of the k according to the relation (21). For example, when $\bar{\sigma}_{s1}=1.1$, $\Delta\bar{z}=0.1$, (the values of other parameters in the Eq. (21) is given above) one can get from the Eq.(21) $k=5.2$.

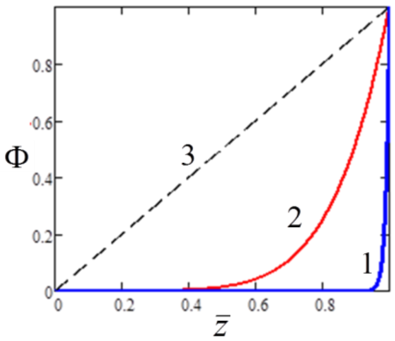

Fig.5 **The dependence $\Phi(\bar{z})=\bar{z}^k$ for different values of the index k : 1- $k=100$, 2- $k=5.2$, 3- $k=1$ (coincide with the velocity field usually used for HPT, uniform strain distribution on the axial direction).**

The dependence $\Phi(\bar{z})=\bar{z}^{5.2}$ is shown in Fig. 5. One can see that in this case the non-uniform torsion covers almost half of the height of the sample. Thus, the formation of a thin layer of hardened material leads to the spread of plastic deformation along the axis of the sample. Moreover, the strain rate in the hardened layer adjacent to the rotary anvil, is significantly reduced. This development of plastic deformation at true constrained HPT follows from the principle of minimum of power dissipation. Since this analysis is based on the Von Mises model, this conclusion is valid for the bulk materials.

The porosity distribution is shown on the Fig.6.

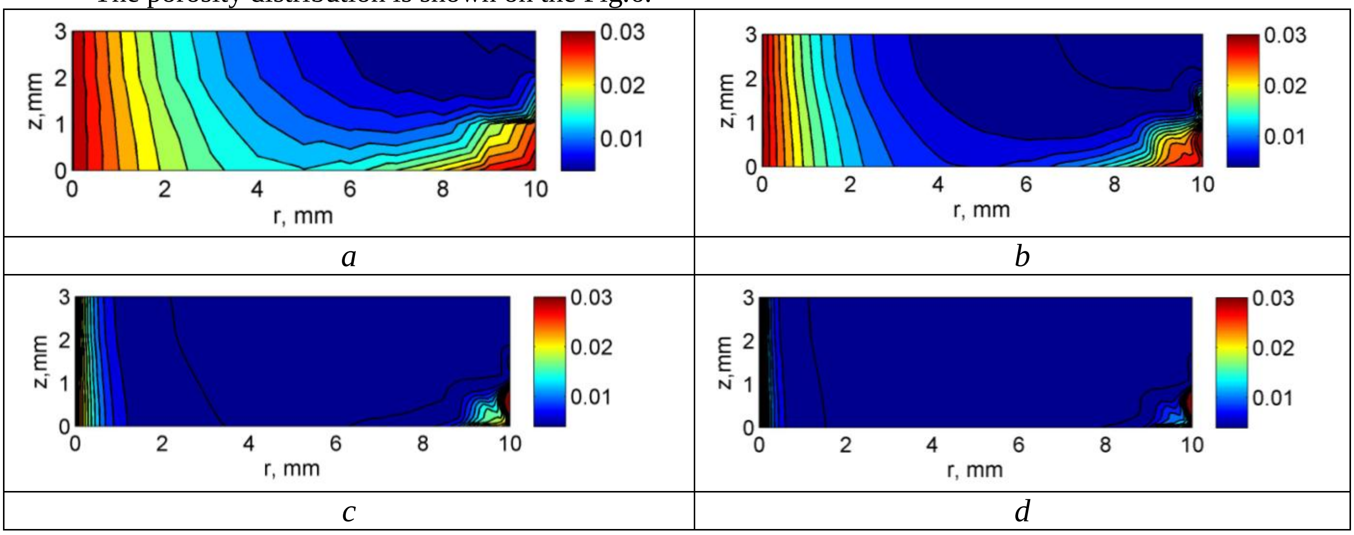

Fig.6 **The porosity distribution for the compression pressure $p=1.1GPa$ and the angles of the anvil rotation equals to: a- $\frac{\pi}{4}$, b- $\frac{\pi}{2}$, c- 2π , and d- 4π .**

This figure shows that the border of the zone with low porosity as well as the border of the zone with the large strain moves in the sample.

It is easy to see that the kinetic Eq. (6) has a steady-state solution

$$\theta_s = -\frac{\alpha}{9a}\frac{\sigma_s}{\sigma}\sqrt{\frac{3}{2}} \tag{18}$$

One can estimate for the condition of the experiment [4] that $\theta_s \approx 0.55\%$

In the Tab. 1 we compare the $\bar{\theta}$ calculated by the Eq.8 with the experimental one [4].

Tab. 1

The average porosity $\bar{\theta}$ after different angle of anvil rotation

Rotation angle	π/2	2π	4π
Porosity (experiment)	2.06	1.01	0.59
Porosity (theory)	1.13	0.60	0.57

The table shows that theory well predicts the steady-state value of the porosity.

Conclusion

By calculating in the commercial DEFORM-2D/3D V11.0 software we shown that the equivalent strain under true constrained high pressure torsion is nonuniform both radially, and axial direction. For homogeneous samples, the deformation is concentrated in a thin layer adjacent to a rotating anvil at the start of the rotation of the anvil. If the material is non-hardened by plastic deformation, the deformation remains localized in a thin layer under further rotation. In contrast, if the material is hardened, the plastic deformation penetrates into the sample with angle of rotation of the anvil increase. The border of a zone with large strain moves both in the radial and axial directions. The above effects are valid for both powder and bulk materials. These effects are associated with friction on the lateral surface of the a cavity of the anvil and follows from the principle of minimum of power dissipation.

The density of the powder material increases with the angle of rotation of the anvil. The border of high density zone moves in the radial and axial directions by increasing of the angle of the anvil rotation. The density in the entire volume of the sample tends to a steady-state value, which decreases with increasing of axial pressure.

References

1. Alexander P. Zhilyaev, Terence G. Langdon, Using high-pressure torsion for metal processing: Fundamentals and applications, Progress in Materials Science, V.53, 6, (2008), 893–979
2. Megumi Kawasaki, Roberto B. Figueiredo, Terence G. Langdon Twenty-five years of severe plastic deformation: recent developments in evaluating the degree of homogeneity through the thickness of disks processed by high-pressure torsion, J Mater Sci (2012) 47:7719–7725
3. Dong Jun Lee, Eun Yoo Yoon, Lee Ju Park, Hyoung Seop Kim, The dead metal zone in high-pressure torsion, Scripta Materialia, V. 67, 4, (2012), 384–387
4. Zhao, Y. J., Massion, R., Grosdidier, T., Toth, L. S., 2014. Contribution of shear deformation to grain refinement and densification of iron powder consolidated by high pressure torsion. In: 6th International Conference on Nanomaterials by Severe Plastic Deformation (NanoSPD6) Book Series: IOP Conference Series-Materials Science and Engineering Volume: 63 Article Number: 012032 .
5. Zhao, Y. J., Massion, R., Grosdidier, T., Toth, L. S., 2015. Gradient Structure in High Pressure Torsion Compacted Iron Powder. Advanced Engineering Materials 17 (12), 1748–1753. A.C.F. Cocks, I.C. Sinka, Constitutive modelling of powder compaction – I.Theoretical concepts, Mechanics of Materials 39 (2007) 392–403
6. L. Resende, J.B. Martin, Formulation of Drucker–Prager Cap Model, J. Eng. Mech. 111 (1985) 855–881.
7. S. Shima, M.Oyane, Plasticity theory for porous metals, Int.J.Mech.Sci. 18 (1976) 285–291.
8. Ja.E. Beigelzimer, B. Efros, V. Varyukhin, A. Khokhlov. A continuum model of a structurally-inhomogeneous porous body and its application for the study of stability and viscous fracture of materials deformed under pressure. Engineering Fracture Mechanics, Vol. 48, No. 5, (1994) 629-640
9. Ya. E. Beigel'zimer, Plastic deformation of porous solids at low porosity, Soviet Powder Metallurgy and Metal Ceramics V. 26, N3 (1987) 193-195
10. Y. Beygelzimer, V. Varyukhin, B. Efros, Physical mechanics of hydrostatic treatment of materials, Donetsk: DonFTI NANU, 192 p., 2000 (in Russian).
11. L. M. Kachanov, Foundations of the Theory of Plasticity (Applied Mathematics and Mechanics, Volume 12), Amsterdam/London 1971. North-Holland Publishing Company
12. DEFORM-2D/3D V11.0

Стаття надійшла до редакції 25.04.2016.